Fang Liu,[1] Dan-Dan Chen,[2] Xin Sun,[3] He-Hui Xie,[2] Hong Yuan,[2] Weiping Jia,[1] and Alex F. Chen[2]

Hydrogen Sulfide Improves Wound Healing via Restoration of Endothelial Progenitor Cell Functions and Activation of Angiopoietin-1 in Type 2 Diabetes

Diabetes 2014;63:1763–1778 | DOI: 10.2337/db13-0483

Impaired angiogenesis and its induced refractory wound lesions are common complications of diabetes. Hydrogen sulfide (H_2S) has been reported to have proangiogenic effects. We hypothesize that H_2S improves diabetic wound healing by restoring endothelial progenitor cell (EPC) function in type 2 diabetes. *db*/*db* Mice were treated with sodium hydrosulfide (NaHS), 4-hydro-xythiobenzamide group (HTB), or saline for 18 days. *db*/+ Mice were treated with DL-propargylglycine (PAG) or saline for 18 days. Plasma H_2S levels were significantly decreased in *db*/*db* mice and restored in the NaHS and HTB mice compared with the diabetic control group. Wound-closure rates were significantly faster in the NaHS and HTB groups than in the *db*/*db* group, in which the PAG group had slower wound-closure rates. Wound skin capillary densities were enhanced in the NaHS and HTB groups. EPC functions were significantly preserved in the NaHS and HTB groups but were decreased in the PAG group. Meanwhile, EPC functions of the *db*/+ mice were significantly reduced after in vitro PAG treatment or cystathionine-γ-lyase (CSE) silencing; EPC functions of *db*/*db* mice were significantly improved after in vitro NaHS treatment. The expressions of Ang-1 in wound skin tissue and in EPCs were upregulated in the NaHS and HTB groups compared with *db*/*db* controls, but were downregulated by in vivo PAG and in vitro siCSE treatment compared with normal controls. Diabetic EPC tube formation capacity was significantly inhibited by Ang-1 small interfering RNA before NaHS treatment compared with *db*/*db* EPCs treated with NaHS only. Taken together, these results show that H_2S improves wound healing by restoration of EPC functions and activation of Ang-1 in type 2 diabetic mice.

Diabetes mellitus and its chronic complications, such as foot problems, are prevalent worldwide. In fact, diabetic foot ulcer is the leading cause of nontraumatic amputation (1). That angiogenesis is crucial for wound healing is well known (2,3). Endothelial progenitor cells (EPCs) play an important role in angiogenesis and neovascularization (4). However, much evidence shows that some aspects of EPC angiogenic ability, as measured by tube formation, adhesion, and migration, decrease in diabetes (5,6). EPC-related angiogenic deficiency induced by diabetes causes chronic vascular complications, refractory wounds, and foot ulcers (3,7,8). Therefore, amendment of EPC function is a critical way to improve wound healing.

Mammalian tissues synthesize hydrogen sulfide (H_2S) by two pyridoxal-5′-phosphate–dependent enzymes catalyzing

[1]Department of Endocrinology & Metabolism, Shanghai Jiao Tong University Affiliated Sixth People's Hospital, Shanghai Clinical Center of Diabetes, Shanghai Institute of Diabetes, Shanghai, China
[2]Department of Cardiology and Center of Clinical Pharmacology, Third Xiangya Hospital, Central South University, Changsha, Hunan, China
[3]Department of Pharmacology, Second Military Medical University, Shanghai, China

Corresponding authors: Alex F. Chen, afychen@yahoo.com; and Weiping Jia, wpjia@sjtu.edu.cn.

Received 31 March 2013 and accepted 26 January 2014.

F.L. and D.-D.C. share first authorship.

the metabolism of L-cysteine: cystathionine β-synthase (CBS) and cystathionine-γ-lyase (CSE), as well as by a recently identified third pathway by the combined action of 3-mercapto-pyruvate sulfurtransferase and cysteine aminotransferase (9,10). H_2S has been considered a poisonous gas for a long time. However, evidence accumulating over the last decade shows that H_2S could act as a novel gasotransmitter and take part in many physiological and pathological processes such as angiogenesis (11), vasodilation (12–14), and inhibition of apoptosis in vascular endothelial cells (15) and cardiomyocytes (16). In the cardiovascular system, the principal enzyme involved in the formation of H_2S is CSE, which converts cystathionine to L-cysteine, yielding pyruvate, ammonia, and H_2S (17). CSE is expressed in vascular endothelial cells, smooth muscle cells, and myocardial cells (18), but to date, whether CSE is expressed in the EPCs is unclear.

Regarding the relationship between H_2S and diabetes, current evidence shows that the synthesis and circulating level of H_2S decreases in NOD mice (19), in streptozotocin-induced type 1 diabetic mice (20), and in type 2 diabetic patients (20). H_2S has been reported to accelerate gastric ulcer healing (21) and healing of burn wounds in the skin (22,23). Papapetropoulos et al. (22) found that topical administration of H_2S improved the recovery from burn wounds in wild-type rats and that genetic ablation of CSE delayed healing in mice. However, little is known about the role of H_2S in chronic skin wound healing in diabetes, especially in type 2 diabetes. Whether H_2S stimulates angiogenesis by influencing the functions of EPCs has also not been elucidated.

Angiopoietin (Ang) plays a major role in endothelial survival and vascular maturation. As a paracrine agonist, Ang-1 can induce phosphorylation of its receptor Tie 2 and promote endothelial survival and vessel stabilization (24). The Ang-1/Tie 2 signal has been reported to contribute to diabetes-induced angiogenesis impairment (25,26), and reduced Ang-1 expression in high-glucose concentration downregulated the phosphatidyl inositol 3-kinase/Akt signaling pathway and phosphorylated endothelial nitric oxide (NO) synthase, which results in the impairment of EPC vessel-forming capacity (25,27). Vascular endothelial growth factor (VEGF) has been reported as a proverbial factor to stimulate angiogenesis and mediate the improving course of wound healing (28,29).

The current study aimed to test our hypothesis that H_2S might improve angiogenesis and restore EPC function in an in vivo wound-healing *db/db* diabetic mouse model. We also investigated the expression of Ang-1 in wound skin tissue and EPCs because it is a possible important factor that mediates the angiogenic effects of H_2S donors. Showing that controlling H_2S can improve wound healing effectively and become a potential strategy for chronic lower extremity ulcerations in diabetic populations would be of great clinical significance.

RESEARCH DESIGN AND METHODS

Experimental Animals and Drugs

All animal procedures were approved by and conducted in accordance with the Central South University Institutional Animal Care and Use Committee established guidelines. The B6.Cg- $m^{+/+}Lepr^{db}/J$ (leptin receptor-deficient diabetes, *db/db*, 8–12 weeks, purchased from The Jackson Laboratory) mouse is a well-established type 2 diabetic animal model with continuous hyperinsulinemia and high plasma glucose levels (30). Their matched nondiabetic littermates (*db/+*) were used as controls.

H_2S was administered in the form of sodium hydrosulfide (NaHS; Sigma-Aldrich) and 4-hydroxylthio-benzamide (4-HTB; Alfa Aesar), which is well established as a reliable H_2S donor (22,31). NaHS is a rapid-releasing H_2S donor widely used in recent in vivo and in vitro H_2S studies (22,23,32), and 4-HTB is a slow-releasing H_2S donor that is effective in improving gastric ulcer healing in rats (21). DL-propargyl-glycine (PAG; Sigma-Aldrich), an irreversible competitive CSE inhibitor, was used to confirm the role of H_2S in *db/+* mice subjected to skin wounding (33,34). Blood glucose from tail veins was measured with a rapid glucose meter (LifeScan One-Touch Ultra 2), and results were expressed as milligrams per deciliter. Diabetes was diagnosed when blood glucose was higher than 300 mg/dL.

Full-Thickness Excisional Dorsal Skin Wounds

Full-thickness punch biopsy wounds were created on male *db/db* mice and their age- and sex-matched *db/+* mice, as we previously described (35,36). Briefly, 6-mm-diameter full-thickness skin wounds were made on the dorsal skin with a biopsy punch (Acuderm Inc., Fort Lauderdale, FL). Wounds were dressed with Tegaderm (Nexcare, 3M) and changed every other day, and wound-closure rates were measured by tracing the wound area every other day onto an acetate paper. Gross wound closure was quantified by Image-Pro Plus 5.1 software (Media Cybernetics), and wound healing was expressed as the percentage of the original wound area that had healed, calculated as $[1 - (\text{wound area day } x/\text{wound area day } 0)] \times 100$.

Animal Groups and Treatment

Mice were randomly assigned to five groups: *db/db* plus NaHS (50 $\mu mol \cdot kg^{-1} \cdot day^{-1}$, $n = 9$), *db/db* plus HTB (30 $\mu mol \cdot kg^{-1} \cdot day^{-1}$, $n = 9$), *db/db* control (saline, $n = 9$), *db/+* control (saline, $n = 10$), and *db/+* plus DL-PAG (50 $mg \cdot kg^{-1} \cdot day^{-1}$, $n = 5$). These drugs were injected intraperitoneally once daily from the day of wounding until 16 days later (22,23,32). At the end of 16 days, or at day 8 after wound creation, mice were killed under isoflurane anesthesia after the blood draw. Blood samples were drawn from the right ventricles by using syringes containing EDTA and then were centrifuged (10,000*g* at 4°C) for 10 min. Thereafter, plasma

was aspirated and stored at −80°C for H_2S concentration measurement. The skin wound tissues were carefully dissected, and granulation tissues within the wound as well as a 10-mm margin of wound were collected.

EPC Therapy for Diabetic Wounds

To determine whether H_2S improves EPC-mediated wound healing in diabetes, 1×10^6 diabetic EPCs were transplanted on *db*/*db* mouse wounds immediately after the skin punch biopsies. Described briefly, one group of *db*/*db* mice (n = 8) received an intraperitoneal injection of NaHS (50 $\mu mol \cdot kg^{-1} \cdot day^{-1}$) every other day until 16 days later, and one group of *db*/*db* mice (n = 8) mice received an intraperitoneal injection of 0.9% saline every other day until 16 days later. These two groups of mice received topical transplants of 1×10^6 diabetic EPCs on wounds, as we described previously (35). Another group of *db*/*db* (n = 8) mice used as a control only underwent skin punch biopsies.

Measurement of H_2S Concentration in Plasma and CSE Activity in Skin Tissue

H_2S in the plasma was determined using previously described methods (37–39). Plasma (120 μL) was mixed with 100 μL water and 120 μL trichloroacetic acid (10% volume for volume), reacted for 10 min at room temperature, and then centrifuged (14,000*g* at 4°C) for 10 min. The clear supernatant was transferred to an Eppendorf tube, then Zn acetate (1%) 60 μL, N,N-dimethyl-p-phenylenediamine sulfate, 40 μL (20 mmol/L in 7.2 mol/L HCl), and $FeCl_3$, 40 μL (30 mmol/L in 1.2 mol/L HCl), were added in proper sequence and reacted for 20 min at room temperature.

For CSE activity assay, the skin tissue was homogenized in an ice-cold 100 mmol/L potassium phosphate buffer (pH 7.4) with an electric homogenizer (PowerGen 125, Fisher Scientific). The homogenate was centrifuged (10,000*g* at 4°C) for 10 min, and the supernatant (430 μL in PBS) was mixed with 20 μL L-cysteine (20 mmol/L), 20 μL pyridoxal-5′-phosphate (2 mmol/L), and 30 μL 0.9% sodium chloride, and reacted for 30 min in a 37°C water bath. Then, 250 μL Zn acetate (1%) and 250 μL trichloroacetic acid (10%) were added to terminate the reaction. After that, N,N-dimethyl-p-phenylenediamine sulfate, 133 μL (20 mmol/L in 7.2 mol/L HCl), and $FeCl_3$, 133 μL (30 mmol/L in 1.2 mol/L HCl), were added. The absorbance of the standards and samples at 670 nm was measured on a spectrophotometer (SpectraMax 190, Molecular Devices) after 20 min. H_2S concentration was calculated against a calibration curve of NaHS (3.125–200 μmol/L) (39). All samples were assayed in duplicate. Results were expressed as plasma H_2S concentration in micromole per liter. The optimal density value of skin samples obtained at 670 nm was adjusted by protein concentration and extrapolated from the standard curve obtained from the same plate. Results of CSE activity were expressed as H_2S concentration in micromoles per microgram of protein.

Isolation and Culture of Bone Marrow–Derived EPCs

EPCs were isolated from the bone marrow of *db*/+ and *db*/*db* mice and cultured afterward according to our established methods with minor modifications (35,40). Described briefly, bone marrow mononuclear cells were isolated from the femurs and tibias of mice by density gradient centrifugation. After two washing steps, mononuclear cells were plated onto vitronectin-coated (Sigma-Aldrich) six-well plates and maintained in endothelial basal medium-2 (Lonza) supplemented with endothelial growth medium 2 (EGM-2, Lonza) with 5% FBS. Cells were cultured at 37°C with 5% CO_2 in a humidified atmosphere. EPCs after 7 days of culture were used for further analysis. To characterize EPCs isolated from bone marrow, stem cell markers (CD34, Sca-1), endothelial cell markers (Flk-1, CD144), and monocyte marker (CD11b) were examined on cultured EPCs by flow cytometry according to our established methods (35,41).

Cytotoxicity Assay

The CellTiter 96 AQ_{ueous} One Solution Cell Proliferation Assay kit (Promega) was used to determine the cytotoxicity of NaHS and PAG in the in vitro studies. Described briefly, 2×10^4 EPCs in 100 μL media were dispensed into each well of 96-well culture plates and cultured overnight. Plates were incubated for 30 min with NaHS (100 μmol/L) or PAG (100 nmol/L). A total of 20 μL of the CellTiter 96 AQ_{ueous} One Solution Reagent containing tetrazolium compound (3-[4,5-dimethylthiazol-2-yl]-5-[3-carboxymethoxyphenyl]-2-[4-sulfophenyl]-2H-tetrazolium, MTS) and an electron coupling reagent (phenazine ethosulfate; PES) was added to each well. Two hours later, the absorbance was recorded at 490 nm using a 96-well plate reader (Molecular Devices, Sunnyvale, CA).

H_2S Treatment by NaHS in Diabetic EPCs

EPCs isolated from *db*/*db* mice were reseeded into six-well plates at 5×10^5 cells/well, incubated at 37°C for 24 h, and serum starved for 8 h. Then they were treated with NaHS at concentrations of 10, 50, and 100 μmol/L in EGM-2 medium for 30 min in a 37°C incubator before function evaluation.

CSE Knockdown by Small Interfering RNA in Normal EPCs

After 7 days in culture, EPCs from *db*/+ mice were reseeded into six-well plates at 2×10^5 cells/well and incubated at 37°C until the cells were 60%–80% confluent. After that, EPCs were serum starved for 6 h before small interfering (si)RNA transfection. The EPC-conditioned media on CSE-siRNA (sc-142618, Santa Cruz Biotechnology) was diluted to a 10 μmol/L working solution and delivered to cells at a 5 nmol/L final concentration through a siRNA transfection reagent (sc-29528, Santa Cruz Biotechnology). After 5–7 h of transfection, the transfection mixture was removed and replaced with fresh EGM-2 and incubated for an additional 48 h. A nonrelated scrambled sequence siRNA (Control siRNA-A, sc-37007; Santa Cruz Biotechnology) was used as a transfection control.

Table 1—Clinical characteristic of participating subjects

	Nondiabetic subjects (n = 8)	Diabetic subjects (n = 7)
Age (years)	40.6 ± 4.3	56.5 ± 7.5
Sex		
Female	3 (37.5)	4 (57.1)
Male	5 (62.5)	3 (43.9)
Fasting plasma glucose (mmol/L)	5.6 ± 0.8	9.1 ± 1.1
Medications	Not applicable	Insulin, acarbose, ACEI, ARB
Comorbidities	Lower extremity traumatic injury	Foot ulcer, peripheral neuropathy, microalbuminuria

Continuous data are presented as mean ± SEM and categoric data as n (%). ACEI, angiotensin-converting enzyme inhibitor; ARB, angiotensin receptor blocker.

CSE Inhibition by DL-PAG in Normal EPCs

EPCs isolated from *db*/+ mice and cultured for 7 days were reseeded into six-well plates at 5×10^5 cells/well and incubated at 37°C for 24 h, then serum starved for 6 to 8 h and treated with DL-PAG at concentrations of 3, 10, and 30 mmol/L in medium for 30 min; the medium containing PAG was then removed and washed twice with PBS for function assay.

Ang-1 Knockdown by siRNA in H_2S-Treated Diabetic EPCs

EPCs isolated from *db*/*db* mice were reseeded into six-well plates at 5×10^5 cells/well, incubated at 37°C for 24 h, and serum starved for 8 h. Then, the EPC-conditioned media on Ang-1 siRNA (Dharmacon) was diluted and delivered to cells at a 5 nmol/L concentration through a siRNA transfection reagent (Dharmacon). After 6 to

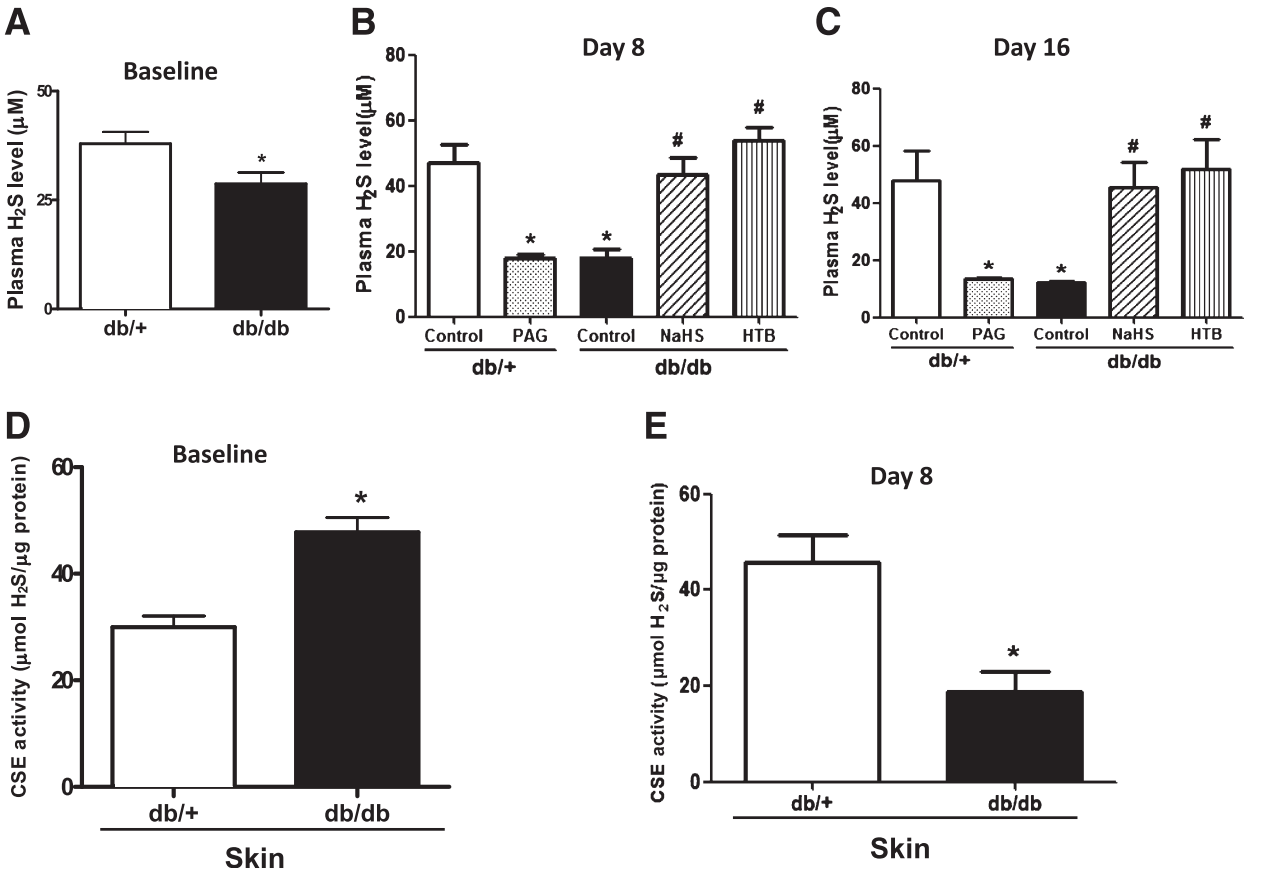

Figure 1—The plasma level of H_2S and CSE activity in wound skin tissue was decreased in diabetic mice, which was reversed by it donors. *A*: Baseline of plasma H_2S level in *db*/+ and *db*/*db* mice (n = 5 each group). *P < 0.05 vs. *db*/+. *B*: Plasma H_2S level at day 8 after wound establishment and H_2S donor or PAG treatment (n = 5 in each group). *P < 0.01 vs. *db*/+ control; #P < 0.01 vs. *db*/*db* control. *C*: Plasma H_2S concentrations at day 16 after wound creation and H_2S donor or PAG treatment (n = 5 each group). *P < 0.05 vs. *db*/+ control; #P < 0.05 vs. *db*/*db* control. *D*: Baseline of the activity of H_2S synthase CSE in the skin tissue of *db*/+ and *db*/*db* mice (n = 5 in each group). *P < 0.05 vs. *db*/+. *E*: There was less CSE activity in the skin tissue of *db*/*db* mice than in *db*/+ mice (n = 5 in each group). *P < 0.01 vs. *db*/+ control.

7 h, the transfection mixture was removed and replaced with fresh EGM-2 and incubated for an additional 48 h before 30-min NaHS treatment at concentration of 50 μmol/L. Of the nonrelated scrambled sequence siRNA–treated *db/db* EPCs, only NaHS 50 μmol/L–treated *db/db* EPCs and the untreated *db/+* EPCs were used as controls. EPC tube formation was assessed after this treatment.

EPC Tube Formation and Adhesion Assays

For the tube formation assay, 48-well plates were coated with growth factor–reduced Matrigel (150 μL/well, Becton, Dickinson and Co.). EPCs (5×10^4), prepared as described above, were plated in 200 μL EGM-2 medium and incubated at 37°C with 5% CO_2 for 12 h overnight to form the tube. Images of tube morphology in a random five fields per well were taken by inverted microscope (Nikon Eclipse TE2000-U) at original magnification ×4 (23). Tube lengths were drawn with Adobe Photoshop CS4 software and analyzed with Image-Pro Plus 5.1 software. For adhesion assay, EPCs were plated at 2.5×10^4/well in triplicate to a vitronectin precoated 96-well plate. After 2 h of incubation at 37°C with 5% CO_2 in EGM-2, nonadherent cells were removed by washing twice with PBS. Cells were fixed with 2% paraformaldehyde (PFA) for 20 min, and the nuclei were stained with Hoechst (5 μg/mL, Sigma-Aldrich) for 20 min. The adherent cells were counted in five random fields in each well with an inverted fluorescence microscope (Nikon) at original magnification ×10, and the mean value of three wells was determined for each sample.

Immunohistochemistry

Capillary density was quantified by histological analysis as previously described (35). At day 8 after wounding, round-shaped 6-mm skin samples, including the healed or unhealed wound area, were fixed with 2% PFA (Sigma-Aldrich), embedded in a cross-section position in paraffin, and sectioned at 4-μm intervals. Slides were deparaffinized and hydrated, blocked with normal rabbit serum (Vector Laboratories) for 30 min, incubated for 60 min at room temperature with an anti-CD31 antibody (1:50; Santa Cruz Biotechnology), and further incubated with Vectastain Elite ABC Reagent (Vector Laboratories) for 30 min and Nova Red (Vector Laboratories) for 15 min. Slides were counterstained with Gill (Lerner) 2 Hematoxylin (VWR Scientific) for 10 s, differentiated in 1% glacial acetic acid, and rinsed in running tap water. Photographs were taken under a Nikon Eclipse TE2000-U microscope using Metamorph software. Five random microscopic fields (original magnification ×20) were counted to determine the number of capillaries per wound, which was expressed as capillaries per high-power field.

Immunofluorescence and Confocal Microscopy

EPCs were isolated as described above and cultured in EGM-2. BrdU staining was performed on EPCs as we

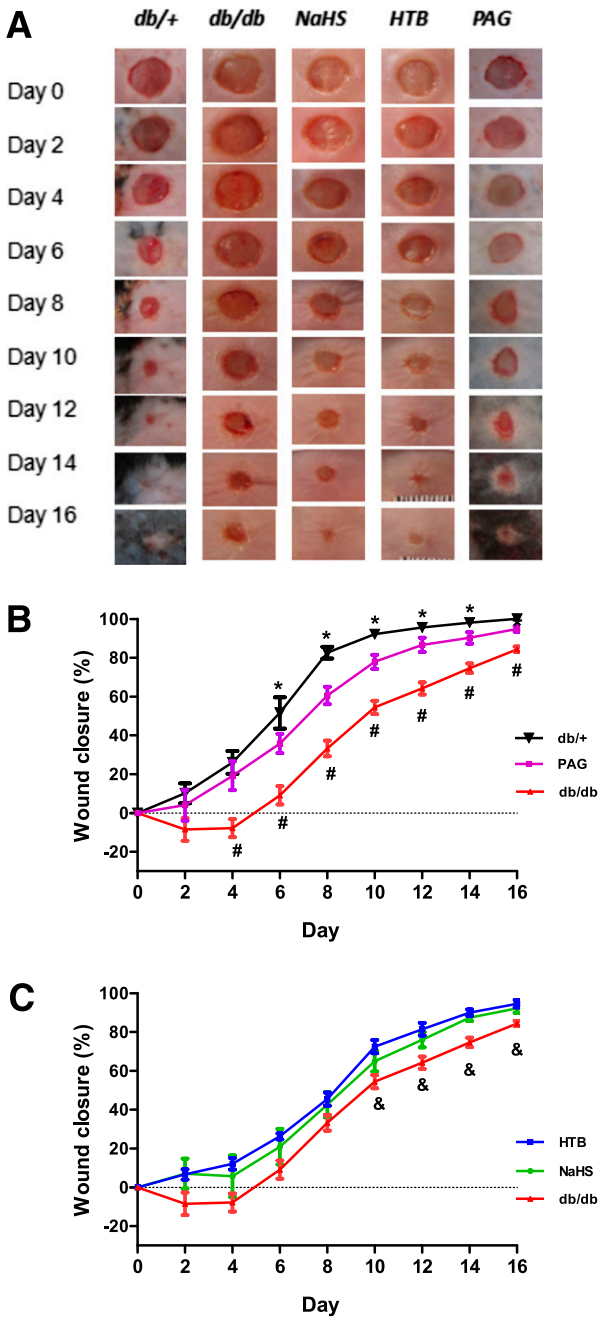

Figure 2—H_2S rapid-releasing (NaHS) and slow-releasing donor (HTB) both accelerated wound healing in diabetic mice, but the CSE inhibitor PAG delayed the wound-closure rate in matched *db/+* controls. Mice were randomly assigned to five groups: *db/db* plus NaHS (50 μmol · kg^{-1} · day^{-1}, n = 9), *db/db* plus HTB (30 μmol · kg^{-1} · day^{-1}, n = 9), *db/db* control (saline, n = 9), *db/+* control (saline, n = 10), and *db/+* plus DL-PAG (50 mg · kg^{-1} · day^{-1}, n = 5). Full-thickness punch biopsy wounds (6-mm diameter) were created on these five groups of mice. Wound-closure rates were measured by tracing the wound area every other day, and gross wound closure was quantified by Image-Pro Plus 5.1. *A*: Photographs show representative wounds with time after wound performance in five groups. *B* and *C*: Comparisons of wound-closure rates in the five groups were expressed by the percentage of closed wound area. *P < 0.05 *db/db* vs. *db/+* or PAG group; #P < 0.05 *db/+* vs. PAG group; &P < 0.05 *db/db* vs. HTB or NaHS group.

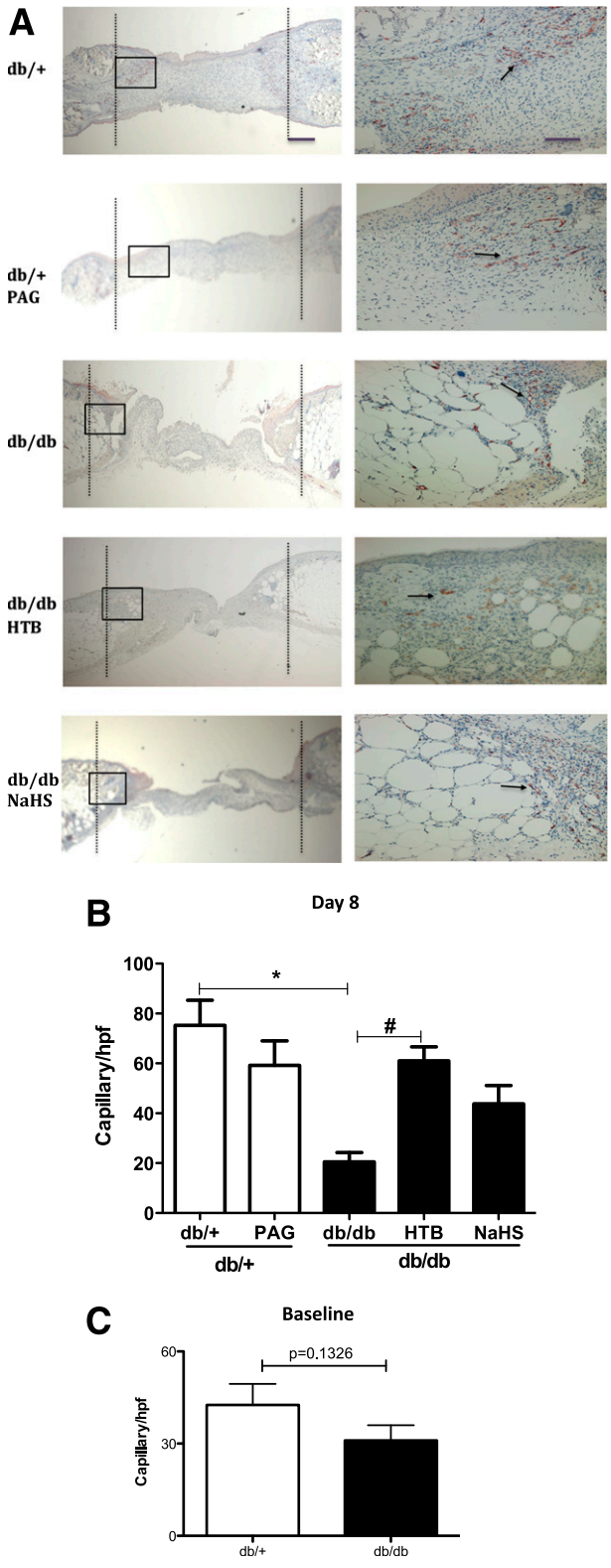

Figure 3—H_2S donor stimulated angiogenesis in wound skin from *db/db* mice. The granule skin tissue within the wound area was collected at day 8 after NaHS, HTB, or PAG treatment and stained with CD31. *A*: Representative photomicrographs of new capillaries in five groups at original magnifications ×4 (*left*) and ×20 (*right*). The black dashed lines indicate the original wound edges, the black boxes indicate the areas enlarged correspondingly in the ×20 magnification panels, and the black arrows point to CD31-positive capillaries. *B*: Comparison of capillary numbers per high-power field (hpf) in five groups ($n = 5$ in each group). *$P < 0.05$ vs. *db/+* control, #$P < 0.05$ vs. *db/db* control. *C*: Comparison of capillary number in unwounded skin in *db/+* mice and *db/db* mice ($n = 5$ each group).

previously described (35). Cultured EPCs were labeled with BrdU and 5-fluro-2′-deoxyuridine (BrdU labeling reagent, Invitrogen). Then, 1×10^6 EPCs were transplanted to 6-mm punch biopsy wounds in *db/db* mice, as described above. On day 8 of wound healing, the mouse was killed, and the wound and surrounding skin was recovered and fixed in 2% PFA for 18 h. Samples were then switched to 70% ethanol. The samples were embedded in paraffin, and 4-mm sections were used for analysis. For staining with rabbit CD31 (1:50; Santa Cruz Biotechnology) and chicken BrdU (1:500; Abcam), primary antibodies were incubated overnight at 4°C. Slides were incubated with Alexa-488 (1:500; Invitrogen Molecular Probes) and Cy3 (1:1,000; Jackson ImmunoResearch Laboratory), followed by 30 s of incubation with Hoechst nuclear stain. Positively stained cells in five random fields were imaged at original magnification ×10 on a Nikon fluorescence microscope (Olympus, Melville, NY). Imaging conditions were maintained at identical settings with original gating performed within each antibody-labeling experiment with the negative control (no primary antibody).

Studies on Type 2 Diabetic Patients

Eight nondiabetic and seven diabetic subjects underwent a full-skin excisional biopsy in their lower extremities. The nondiabetic subjects were recruited from patients admitted to the Division of Vascular Surgery of Shanghai Clinical Center because of traumatic wounds and did not have cardiovascular, renal, or hepatic disease. The diabetic subjects were recruited from Shanghai Clinical Center of Diabetes, and those who had foot or leg ulceration and underwent the debridement operation in our Division of Vascular Surgery were included in the study. The clinical characteristics of participating subjects are outlined in Table 1. All lower limb skin biopsies were performed during the limb operation by surgeons, and the skin beside the wound (margin within 1 cm) was taken. Protocols were approved by the institutional review boards of Shanghai Jiao Tong University and the Shanghai Clinical Center of Diabetes. Written informed consent was obtained from every subject. The skin tissues were used to examine the expressions of Ang-1, CSE, and VEGF by Western blot.

Western Blot Analysis

Total protein was extracted from cultured EPCs after in vitro culture and treatment, as described above, or from harvested wound skin tissue, including a 6-mm region of skin located in the wound and 10 mm of skin tissue around the wound bed, by homogenization of skin wounds in tissue lysis buffer (Sigma-Aldrich). Protein

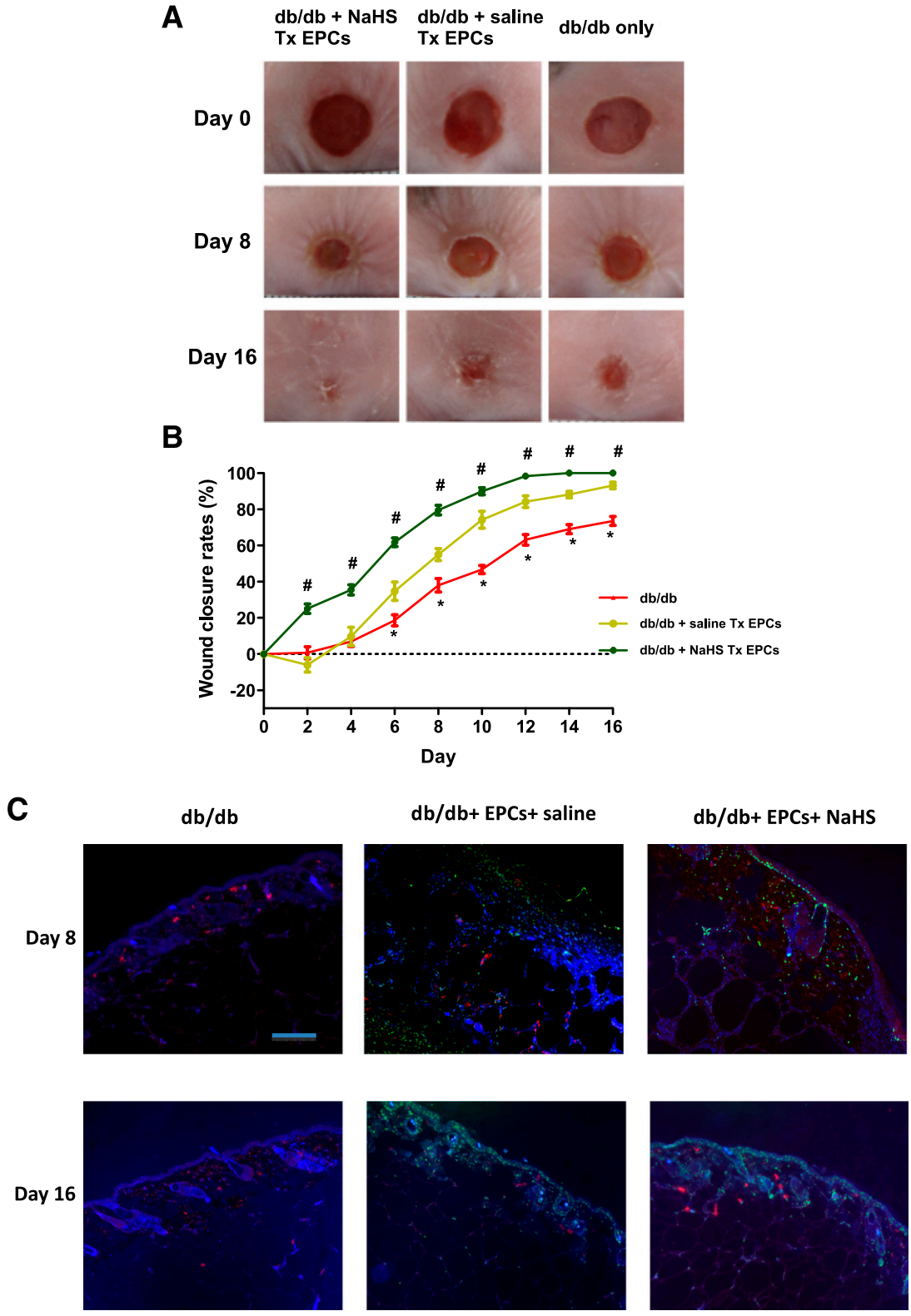

Figure 4—H_2S donor accelerated the rate of EPC-mediated wound healing in diabetic mice. One group of *db*/*db* mice (n = 8) received an intraperitoneal injection of NaHS (50 μmol · kg^{-1} · day^{-1}) every other day for 16 days (*db*/*db* + NaHS Tx EPCs), and one group of *db*/*db* mice (n = 8) mice received an intraperitoneal injection of 0.9% saline every other day for 16 days (*db*/*db* + saline Tx EPCs). These two groups of mice received topically transplanted (Tx) 1 ×10^6 diabetic EPCs on wounds immediately after skin punch biopsies. Another group of *db*/*db* mice (n = 8) used as control only underwent skin punch biopsies (*db*/*db* only). *A*: Photographs of representative wounds, with time after wound performance, in the three groups. *B*: Comparisons of the wound-closure rates in the three groups were expressed by the percentage of closed wound area. *P < 0.05 *db*/*db* vs. *db*/*db* + NaHS Tx EPCs or *db*/*db* + saline Tx EPCs; #P < 0.05 *db*/*db* + NaHS Tx EPCs vs. *db*/*db* + saline Tx EPCs. *C*: Representative photographs demonstrated EPC integration into the dermis and vascular structure. On

concentration was determined by a bicinchoninic acid protein assay kit (Pierce). Equal amounts of proteins (30–50 μg) were boiled and separated by 6–12% SDS-PAGE and transferred onto nitrocellulose membrane (Amersham Hybond-ECL, GE Healthcare). CSE (mouse monoclonal anti-CSE, Santa Cruz Biotechnology), CBS (mouse monoclonal anti-CBS, Santa Cruz Biotechnology), and Ang-1 (rabbit polyclonal anti–Ang-1, Abcam) were determined with its specific first antibodies. The dilutions of primary antibody were 1:500 for Ang-1, 1:10000 for β-actin (Santa Cruz Biotechnology), and 1:250 for all other antibodies. Luciferin-conjugated secondary antibody was used at 1:5000. The bands were scanned and analyzed by the Odyssey system.

Statistical Analysis

Results are expressed as mean ± SEM. Differences between the two groups were compared with paired or unpaired Student *t* tests. One-way ANOVA with Tukey multiple comparison tests were used to compare each parameter when there were two or more independent groups. Two-way ANOVA of grouped analyses was used to compare the wound recovery rate at different time points, and then Bonferroni post hoc *t* tests were performed to compare replicate means by row when ANOVA was statistically significant. Values of $P < 0.05$ were considered statistically significant.

RESULTS

H_2S Donor Therapy Corrected Decreased Plasma Concentration of H_2S and CSE Activity in Diabetic Mice Skin Tissue

At 8–10 weeks of age, the body weights of the *db*/*db* mice were significantly greater than those of the *db*/+ mice (40.06 ± 3.37 g vs. 25.99 ± 1.22 g; $P < 0.01$), and the blood glucose levels of the *db*/*db* mice were significantly higher than those of the *db*/+ mice (475.89 ± 42.27 mg/dL vs. 139.9 ± 33.49 mg/dL; $P < 0.01$). The baseline plasma H_2S concentration of the *db*/+ mice was significantly higher than that of the *db*/*db* mice (Fig. 1*A*). The plasma H_2S concentrations of the *db*/*db* mice were further decreased than those of *db*/+ mice after wound creation and were reversed by NaHS and HTB at day 8 (Fig. 1*B*) and day 18 (Fig. 1*C*). In contrast, PAG downregulated the H_2S plasma concentrations in the *db*/+ mice (Fig. 1*B* and *C*). Although the baseline level of H_2S synthase CSE activity in the skin tissue of *db*/*db* mice was higher than in that of the *db*/+ mice (Fig. 1*D*), the CSE activity of the *db*/*db* mice was significantly lower compared with that of the *db*/+ mice after wound creation at day 8 (Fig. 1*E*).

H_2S Therapy Accelerated Wound Healing in Diabetic Mice

The baselines of wound healing in *db*/*db* and *db*/+ mice were determined. The data demonstrated that the wound areas of the *db*/*db* mice closed significantly slower than those of the *db*/+ mice from day 2 to day 16 (Fig. 2*A* and *B*). The administration of the rapid-releasing NaHS or slow-releasing HTB H_2S donor improved wound recovery rates compared with saline-treated *db*/*db* controls (Fig. 2*B* and *C*) starting from day 2 to day 16. The overall wound-healing rate in the two H_2S donor groups was still slower than that of the *db*/+ group (Fig. 2*B* and *C*). In contrast, the administration of H_2S synthase CSE inhibitor, DL-PAG, significantly delayed the wound closure rate compared with the *db*/+ group (Fig. 2*B* and *C*). These data suggest that H_2S treatment improved wound healing in type 2 diabetic mice, whereas the inhibition of H_2S synthesis in vivo delayed the wound-healing course.

Slow-Releasing H_2S Donor Stimulates Angiogenesis of Wound Skin Tissue

At day 8 after treatments, capillary numbers in the diabetic group were significantly lower than those in the normal control group (Fig. 3*A* and *B*). The slow-releasing H_2S donor HTB significantly increased the newly formed capillary densities compared with that of diabetic controls (Fig. 3*A* and *B*), whereas the vessel densities in skin tissue treated by NaHS augmented the newly formed capillary densities to some extent but without reaching statistical significance. On the contrary, new vessel densities were lower in wound skin taken from mice treated with PAG than from wound skin taken from normal *db*/+ controls (Fig. 3*A* and *B*). The difference in the baselines of capillary numbers of unwounded skin between *db*/+ mice and *db*/*db* mice was not significant (Fig. 3*C*).

H_2S Donor Accelerated the Rate of EPC-Mediated Wound Healing in Diabetic Mice

Wound healing improved significantly in the diabetic mice that received EPC transplantation. Furthermore, NaHS significantly augmented the efficiency of EPC cell therapy in diabetic mice ($P < 0.05$ vs. *db*/*db* mice; Fig. 4*A* and *B*). These data suggest that H_2S significantly accelerated EPC-mediated wound healing in diabetic mice. On day 8 of wound beds, some BrdU-labeled EPCs integrated into vascular-like structures (CD31-positive) and the other BrdU-labeled EPCs integrated in the dermis. On day 16 of wound beds, more BrdU-labeled cells integrated into the epithelial layers (Fig. 4*C*).

day 8 of wound beds, some BrdU-labeled EPCs (green fluorescence) integrated into vascular-like structures (CD31-positive, red fluorescence), and the other BrdU-labeled EPCs integrated in the dermis. On day 16 of wound beds, more BrdU-labeled EPCs integrated into the epithelial layers. The nuclei were counterstained with DAPI (blue fluorescence). The merged image is shown in *C*. The skin sample was imaged at original magnification ×10 using a Nikon 90i upright microscope. Scale for ×10 = 200 μm.

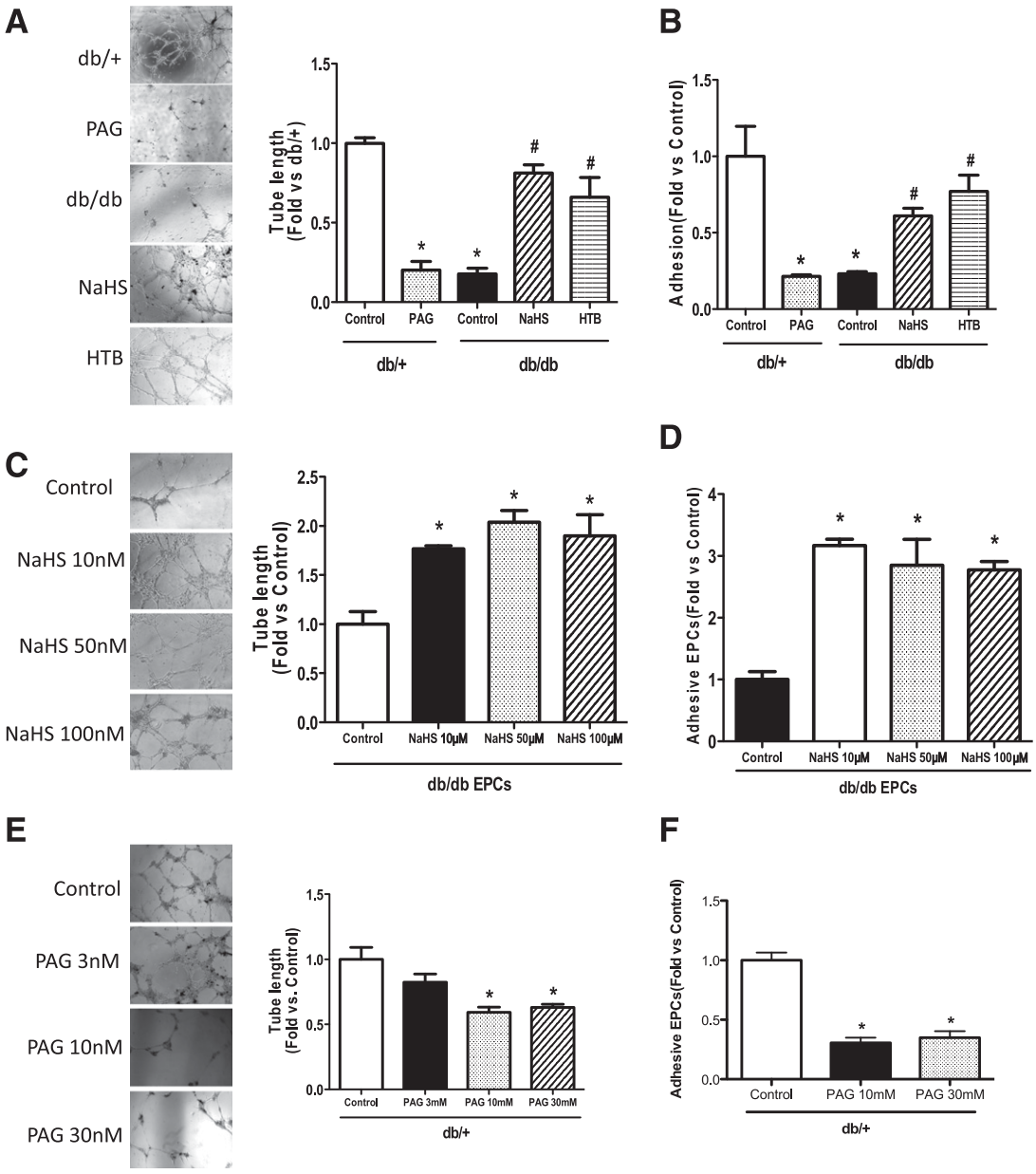

Figure 5—H_2S donor restored the EPC functions of diabetic mice in vivo and in vitro, whereas H_2S inhibition suppressed the angiogenic functions of normal EPCs. EPCs were isolated from the bone marrow of five groups after 16 days of in vivo treatment and cultured in EGM-2 for 7 days before assay or collected directly from *db/db* or *db*/+ mice. The reseeded EPCs (5×10^5) were treated in vitro with NaHS 10, 50, or 100 μmol/L in EGM-2 for 30 min; PAG 3, 10, or 30 mmol/L in EGM-2 for 30 min; or CSE-siRNA at 50 nmol/L in medium for 6–7 h after 6–8 h of serum starvation before tube formation on Matrigel and adhesion assay. *A*: Representative tube network photographs under a microscope (original magnification ×4) and comparison of tube length among five groups after 16 days of in vivo treatment of H_2S donor (n = 4–5). *P < 0.01 PAG vs. *db*/+ control, *db/db* vs. *db*/+; #P < 0. 01 NaHS vs. *db/db*, HTB vs. *db/db* control. *B*: Comparison of adhesive cell numbers of five groups (n = 3–5). *P < 0.01 *db/db* vs. *db*/+, PAG vs. *db*/+ control; #P < 0.01 NaHS vs. *db/db* and HTB vs. *db/db* control. *C*: Photographs of representative tube networks under microscope (original magnification ×4) and comparison of tube length in four groups treated with different NaHS concentrations and controls (n = 3–4). *P < 0.01 vs. *db/db* control. *D*: Comparison of the adhesive EPC numbers of four groups treated with different NaHS concentrations and controls (n = 5). *P < 0.01 vs. *db/db* control. *E*: Representative photographs of tube networks under microscope (original magnification ×4) and comparison of mean tube length in four groups with in vitro PAG at 3, 10, or 30 mmol/L treatment (n = 5 each group). *P < 0.01 vs. control. *F*: Comparison of adhesive cells numbers in four groups with different concentrations of PAG treatment (n = 4). *P < 0.01 vs. *db*/+ control. *G*: CSE silencing with CSE-siRNA in normal EPCs inhibited the CSE expression by 70% in siCSE transfected EPCs (n = 4–5). *P < 0.01 vs. control. *H*: CSE silencing did not alter the CBS expression of normal EPCs. P > 0.05 vs. control. *I*: The tube length of EPCs after CSE silencing decreased by nearly 40% (n = 7 in each group). *P < 0.01 vs. control. *J*: The adhesive EPC numbers decreased by 55% in CSE-silenced EPCs (n = 4 in each group). *P < 0.01 vs. control. *K*: Cell viability was not affected by 100 μmol/L NaHS or 30 mmol/L PAG (n = 4–5). P > 0.05.

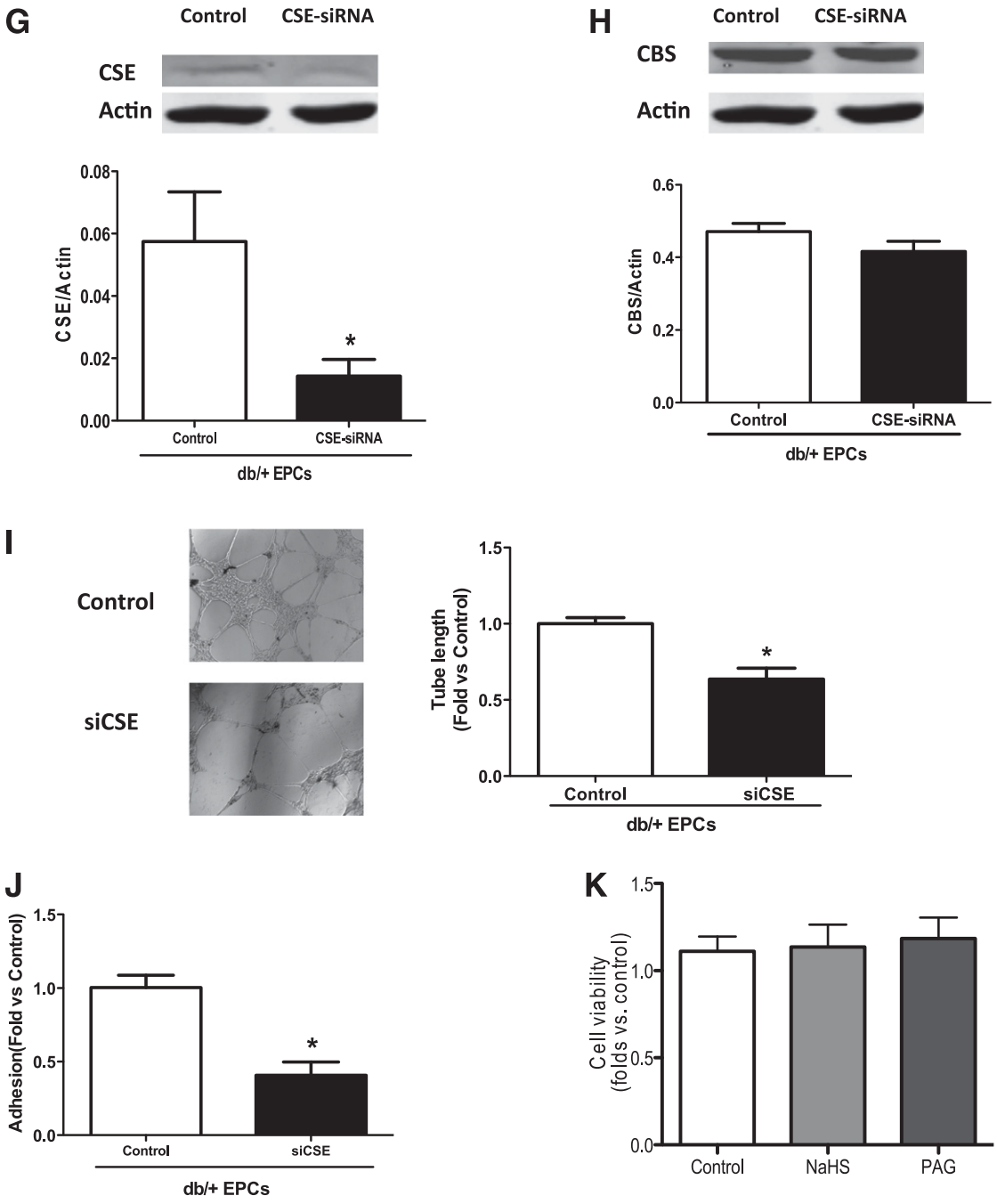

Figure 5—*Continued*

H_2S Donor Improved Tube Formation and Adhesive Function of Diabetic EPCs

To investigate the functions of EPCs, EPC tube formation on Matrigel and EPC adhesion in vitronectin precoated plates were observed in EPCs isolated from mice after 16 days of treatment with H_2S or PAG. The cell population profiles of cultured EPCs (day 7) were as follows: Sca-1 (60.8 ± 7.52%), CD34 (47.6 ± 4.37%), Flk-1 (22.6 ± 3.17%), CD144 (8.7 ± 1.19%), and CD11b (37.5 ± 2.54%), indicating that 7-day cultured EPCs are heterogeneous populations containing both higher percentages of stem cells and endothelial cells. The *db/db* EPCs formed significantly fewer tube networks than the *db/+* EPCs (Fig. 5*A*). In vivo H_2S therapy with NaHS and HTB significantly improved the ability of diabetic EPCs to form tube networks compared with *db/db* control EPCs (Fig. 5*A*). On the contrary, PAG treatment significantly reduced the tube length compared with normal controls (Fig. 5*A*). Similar to tube formation, the adhesive numbers

of EPCs in the *db*/*db* group was markedly less than that in the normal group (Fig. 4*B*), and administration of NaHS and HTB significantly increased the adhesion function of EPCs compared with untreated *db*/*db* EPCs (Fig. 5*B*). Contrarily, EPC adhesion in the PAG group was significantly attenuated compared with that of the *db*/+ control group (Fig. 4*B*).

To observe the influence of H_2S on the functions of diabetic EPCs in vitro, EPCs isolated from the bone marrow of *db*/*db* mice were treated with NaHS at concentrations of 10, 50, and 100 μmol/L in EMG-2 for 30 min before tube formation and adhesion determination. NaHS significantly augmented the tube networks of diabetic EPCs at all three concentrations compared with nonmodified *db*/*db* EPCs (Fig. 5*C*). The deficient adhesion of diabetic EPCs was also reversed by NaHS with concentrations of above 10 μmol/L in vitro (Fig. 5*D*). These aforementioned data suggest that in vivo and in vitro H_2S donor treatment both restore deficient EPC tube formation and adhesive functions in *db*/*db* mice.

H_2S Inhibition With DL-PAG and CSE siRNA Reduced the Function of Normal EPCs In Vitro

To verify whether H_2S inhibition could impair EPC function, H_2S synthesis of EPCs was inhibited with different concentrations of DL-PAG (3, 10, and 30 mmol/L), which was added to EGM-2 medium for 30 min. The results indicated that the tube length of EPCs treated with PAG 10 mmol/L and 30 mmol/L decreased significantly compared with that of normal controls (Fig. 5*E*). Similarly, the adhesive EPC numbers were reduced markedly in the PAG 10 mmol/L and 30 mmol/L intervention groups compared with control EPCs (Fig. 5*F*). These results suggest that the inhibition of H_2S synthesis in EPCs reduces their functions.

The tube formation results from the CSE silencing experiment in EPCs further demonstrated the critical effect of H_2S on EPC angiogenesis. The CSE expression of EPCs after siCSE treatment was reduced by nearly 70%, as shown by Western blotting (Fig. 5*G*), whereas the expression of CBS was not influenced by the silencing of CSE in EPCs (Fig. 5*H*). The average tube length of EPCs after CSE knockdown decreased to ~40% compared with controls (Fig. 5*I*), and EPC adhesion also was markedly attenuated compared with controls (Fig. 5*J*). These data identified that H_2S is critical for EPC functions, including tube formation and adhesion abilities. In addition, the cytotoxicity assay showed that treatment with NaHS or PAG did not affect the viability of EPCs (Fig. 5*K*).

H_2S Donor Upregulated Expressions of Ang-1 in Wound Skin Tissues and EPCs of Diabetic Mice, Whereas CSE Suppression Downregulated Ang-1 Expression in Normal EPCs

To understand the possible mechanism through which H_2S improves EPC function, the expressions of Ang-1 and VEGF in wound skin tissue and EPCs were measured by Western blotting. The results indicated that the in vivo H_2S donor treatment significantly increased the expressions of Ang-1 and VEGF not only in EPCs from these mice but also in wound skin tissues (Fig. 6*A*–*C*). On the contrary, the CSE inhibitor PAG inhibited the expression of Ang-1 in the wound skin tissue (Fig. 6*A*) and in EPCs (Fig. 6*B*). Similarly, the silencing of CSE in cultured normal EPCs with CSE siRNA in vitro treatment significantly decreased their Ang-1 expression (Fig. 6*D*).

H_2S Promoted Angiogenesis of EPCs by Restoration of Ang-1 Expression

To identify whether H_2S stimulates the angiogenic function of EPCs through Ang-1 signaling, EPCs were pretreated with Ang-1 siRNA before in vitro NaHS treatment. EPCs were isolated from the bone marrow of *db*/*db* and normal mice and cultured in EGM-2 for 7 days. Diabetic EPCs (5×10^5) were then reseeded and treated in vitro with NaHS at 50 μmol/L only in EGM-2 for 30 min or with Ang-1 siRNA at 5 nmol/L in medium for 6–7 h before NaHS treatment. The results revealed that the improved tube length with NaHS was significantly inhibited by prior Ang-1 siRNA treatment and was significantly lower than that of normal EPCs (all $P < 0.05$; Fig. 7*A* and *B*). These results suggest that H_2S exerts its role of promoting EPC angiogenesis, at least partially, by restoration of Ang-1.

Expressions of Ang-1, CSE, and VEGF Were Decreased in the Human Skin Tissue of Diabetic Foot Ulcers

To investigate whether the dysregulations of Ang-1, CSE, and VEGF also applied to the skin tissue from foot ulcers of diabetic subjects, we compared their expression between nondiabetic and type 2 diabetic subjects. The data showed that the expressions levels of Ang-1, CSE, and VEGF were 36%, 41%, and 46% lower, respectively, in the diabetic subjects compared with the nondiabetic subjects (Fig. 8).

DISCUSSION

H_2S is the "third" gasotransmitter next to NO and carbon monoxide (CO). Its biological effects have not yet been completely understood. The current study demonstrates that *1*) plasma H_2S levels and CSE activities in skin wounds decreased in type 2 diabetic mice; *2*) in vivo and in vitro H_2S treatment both amended the tube formation and adhesive functions of diabetic EPCs; *3*) H_2S donor therapy improved EPC-mediated wound healing in diabetic mice via elevating angiogenesis; *4*) H_2S treatment increased the expression of Ang-1 and VEGF in EPCs from diabetic mice and Ang-1 siRNA inhibited the ameliorative effect of NaHS on EPC angiogenic functions; and *5*) the expressions of Ang-1, CSE, and VEGF were decreased in diabetic ulcers in diabetic patients.

The baselines of plasma H_2S in diabetic mice were significantly lower than those of the nondiabetic mice, which is consistent with the plasma H_2S measurements in NOD mice (19) and streptozotocin-induced type 1 diabetic mice (20). On day 8 or day 16 after skin wounds, the plasma H_2S levels were further decreased in the diabetic

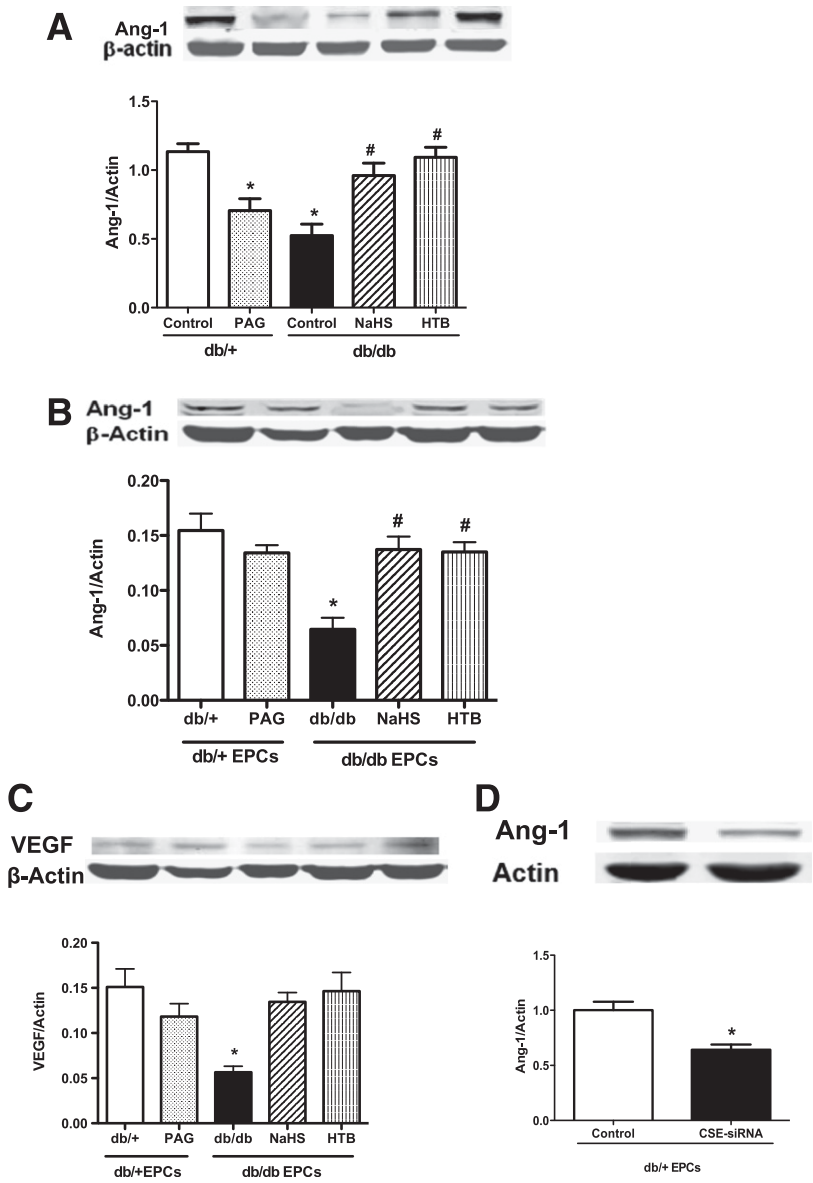

Figure 6—H_2S donor upregulated the expressions of Ang-1 in wound skin tissues and in EPCs in type 2 diabetes, whereas CSE suppression downregulated Ang-1 expression in normal EPCs. Protein was extracted from 6 mm of wound skin and 0.5 cm of skin outside of the wound, and 7-day cultured EPCs after 16 days of in vivo treatment by two H_2S donors and PAG, or normal EPCs with in vitro CSE siRNA 50 nmol/L treatment and its controls. *A* and *B*: Protein bands and comparison of EPCs and skin tissue Ang-1 expression in five groups (n = 4–5). *P < 0.01 PAG vs. *db*/+ control, *db*/*db* vs. *db*/+ control; #P < 0.01 NaHS vs. *db*/*db* control and HTB vs. *db*/*db* control. *C*: Protein bands and comparison of VEGF expression of EPCs in five groups (n = 4–5). *P < 0.01 *db*/*db* vs. *db*/+. *D*: Protein bands and comparison of Ang-1 expression in EPCs with and without CSE siRNA treatment (n = 4–5). *P < 0.01 vs. control.

mice, whereas the plasma H_2S levels in the nondiabetic mice were maintained at baseline level. Interestingly, the baseline activity of CSE in skin tissues was ~1.3-fold higher in the diabetic mice than in the nondiabetic mice, which might be a compensative response to decreased plasma H_2S levels. However, on day 8 after wounds, CSE activity in skin wounds of the diabetic mice was significantly attenuated and failed to produce enough H_2S for wound healing, whereas CSE activity in the nondiabetic skin wounds was higher than at baseline, which might be a mechanism for the unchanged H_2S levels. Because the expression of another H_2S synthase, CBS, was not changed in skin tissue and in the EPCs of diabetic mice, the delayed wound healing in diabetic mice is more likely due to the deficiency of H_2S synthesis in the vascular system, just as Brancaleone et al. (19) reported in NOD mice.

H_2S had been found to improve the burn skin wound and gastric ulcers induced by acetate acid in wild-type mice or rats (18–20) and to improve endothelial wound healing in an in vitro model (23). Wallace et al. (21) revealed an enhancing effect of H_2S in acetic acid–induced

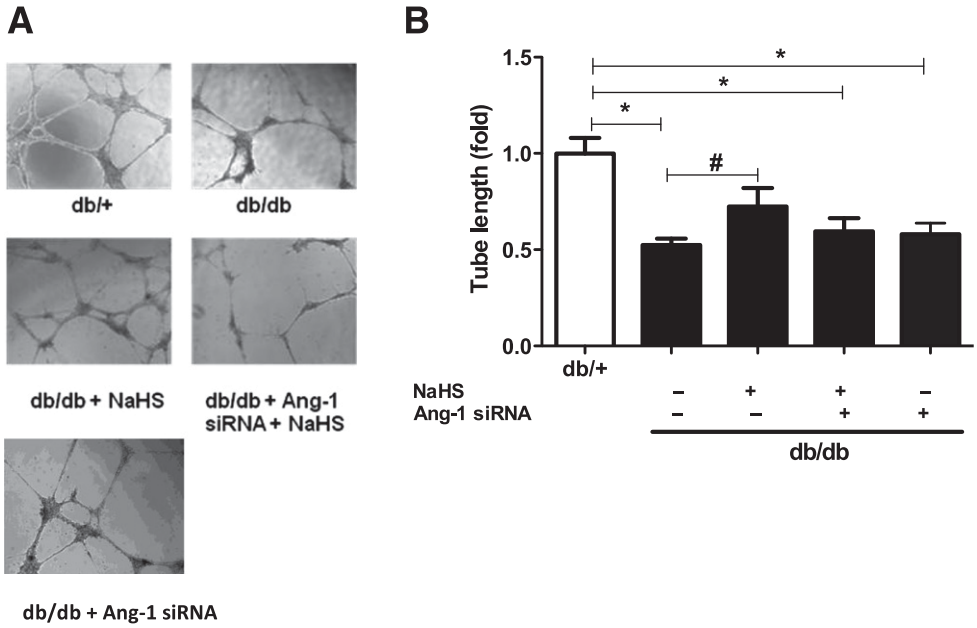

Figure 7—H_2S promoted EPC angiogenesis by restoration of Ang-1 expression. EPCs were isolated from bone marrow of *db/db* and normal mice and cultured in EGM-2 for 7 days, then *db/db* EPCs (5×10^5) were reseeded and treated in vitro with NaHS 50 nmol/L only in EGM-2 for 30 min, or Ang-1 siRNA at 5 nmol/L in medium for 6–7 h before NaHS 50 nmol/L treatment. Then, tube formation on Matrigel and adhesion on vitronectin assay were performed in all EPCs. *A*: Representative photographs of tube networks under microscope (original magnification ×4). *B*: Comparison of tube length in four groups of *db*/+ EPCs and *db/db* EPCs treated with and without NaHS, NaHS and Ang-1 siRNA (n = 4 in each group). *P < 0.05 vs. *db*/+, #P < 0.05 vs. *db/db* only.

gastric ulcers in a Wistar rat model and in a skin burn wound model in CSE-knockout mice (22). This evidence suggests that H_2S contributes to wound healing. However, no evidence of its efficacy on diabetic wounds has been reported so far.

In the current study, two H_2S donors, NaHS and 4-HTB, were administrated in vivo; the first is the widely used rapid-releasing donor and the latter is the slow-releasing H_2S donor. The usual dosage NaHS range is 10–100 μmol/kg, as reported in recent in vivo studies (22,23,32). On the basis of this evidence and considering that the physiological H_2S levels in the plasma of mammals were 10–100 μmol/L (42), we chose 50 μmol/kg as the treatment dosage of NaHS in the current study. As for 4-HTB, only one experience, reported by Wallace et al. (21), could be referenced. They used HTB 10–30 μmol/kg twice daily by intragastric administration in male Wistar rats (21), so we administered the dose of 30 μmol/kg to diabetic mice and proved its efficacy on diabetic wound healing. The results of this study demonstrate that an intraperitoneal injection of the H_2S donors NaHS and 4-HTB both improved the recovery rate of wound healing in type 2 diabetic mice and had similar effects on wound healing in diabetic mice. Because NaHS and 4-HTB are easily available H_2S donors, they may be potential remedies to ameliorate foot ulcerations in diabetic patients.

Insufficient angiogenesis is one of most important reasons for delayed diabetic wound healing. The prominent functions of EPCs in angiogenesis have been widely demonstrated (35,43,44). In the current study, the tube formation and adhesive function of diabetic EPCs was impaired compared with normal mice with a matched genetic background, suggesting that their angiogenic effect was attenuated. The proangiogenic effect of H_2S has been recently recognized. Cai et al. (23) reported a novel Akt-mediated proangiogenic role of H_2S in C57BL/6 mice. Topical administration of H_2S enhanced wound healing in CSE knockout mice, and the researchers concluded that endogenous H_2S stimulates endothelial cell–related angiogenic properties through a ATP-sensitive K^+ channel/mitogen-activated protein kinase pathway (22). H_2S also enhances tube formation and migration in cultured vascular endothelial cells (32). The current study demonstrated that H_2S donors facilitated diabetic wound healing by stimulating capillary formation at the site of injury. Furthermore, we demonstrated that the H_2S donor accelerated EPC-mediated wound healing in diabetic mice. To date, whether H_2S ameliorates diabetic wound healing by influencing EPC functions has not been elucidated.

In the current study, we first investigated the angiogenic effects of H_2S donors on EPCs isolated from diabetic mice in vitro. Our results revealed that the tube formation and adhesion of EPCs increased significantly by chronic treatments with both the rapid-releasing and slow-releasing H_2S donor in diabetic mice. Furthermore, the angiogenic function of diabetic EPCs also was restored by NaHS in vitro. These results support that H_2S improves the angiogenic function of diabetic EPCs. On

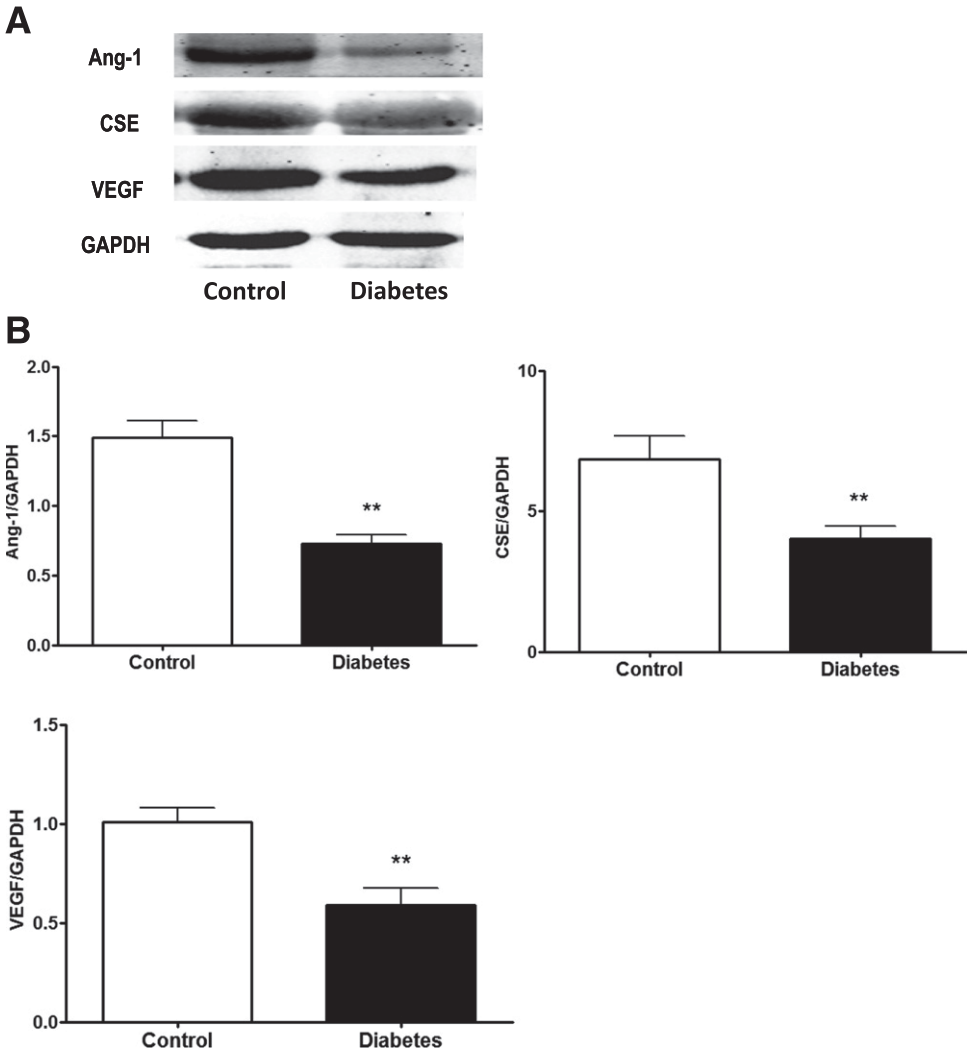

Figure 8—The expressions of Ang-1, CSE, and VEGF were decreased in human skin tissue of diabetic foot ulcers. *A*: Representative protein bands of Ang-1, CSE, and VEGF of skin tissue. *B*: The expression of Ang-1, CSE, and VEGF were lower in the foot ulcer skin tissue of diabetic patients than in nondiabetic controls (n = 7–8 in each group). $^{**}P < 0.05$ vs. control. GAPDH, glyceraldehyde-3-phosphate dehydrogenase.

the contrary, after the normal mice and their EPCs were treated with the H_2S synthetase (CSE) inhibitor DL-PAG in vivo and in vitro, or siCSE in vitro, the tube network formation and adhesive ability of normal EPCs declined markedly at the same time the wound closure rate was delayed. We have demonstrated that topical EPCs transplantation significantly improves wound healing in the diabetic mice (35,45). In the current study, we found that NaHS significantly augmented the efficiency of EPC cell therapy in diabetic mice. Consistent with our previous studies, some EPCs integrated into vascular-like structures and the other EPCs integrated in the dermis at the early stage of wound beds (on day 8), indicating that H_2S accelerates wound healing by EPC-mediated angiogenesis. Interestingly, we also found that more cells integrated into the epithelial layers at the later stage of wound beds (on day 16), which may be investigated in future studies. In vitro and in vivo evidence both suggests that H_2S is vital for preserving normal EPC functions and wound repair in type 2 diabetic mice.

Angiogenic signals are mainly activated by endothelium-specific receptor tyrosine kinase, of which VEGF, fibroblast growth factor, and Ang-1 are ligands. Ang-1 promotes endothelial differentiation from embryonic stem cells and induces pluripotent stem cells (46). Ang-1 gene expression was downregulated in EPCs cultured in a high glucose environment, and recombinant Ang-1 increased the vessel-forming capacity of EPCs in vitro (47). The current study showed that in vivo treatment with H_2S donors significantly increased the expressions of Ang-1 and VEGF in EPCs from diabetic mice. Most importantly, we also found attenuated expression of Ang-1 and VEGF in diabetic wounds in patients. Although the current study cannot exclude the effects of sex, medications, and comorbidities on the expressions of Ang-1, CSE, and VEGF, our results provided evidence that angiogenic

factors and H_2S were significantly attenuated in local diabetic wounds, which may contribute to refractory wounds in diabetic patients. Ang-1 was reported to potentiate VEGF-induced angiogenesis (48). Ang-1 signaling was known to regulate vascular quiescence and angiogenesis through its cognate receptor Tie-2 (49). However, we did not observe altered expression of the Ang-1 receptor Tie-2 between diabetic EPC or diabetic wounds. In parallel, the tube formation and adhesion ability of H_2S-amended EPCs increased significantly, which was blocked by pretreatment by Ang-1 siRNA before H_2S. These results suggest that the restoration of EPC angiogenic functions by H_2S may occur, at least partly, through the mediation of Ang-1. H_2S activates phosphatidylinositol-3-kinase and mitogen-activated protein kinases to regulate angiogenic factors in endothelial cells (22,50,51). However, the mechanisms by which H_2S regulates Ang-1 in EPCs are still unknown. Further research should be done to clarify how and to what degree H_2S improves diabetic wound healing and EPC function via Ang-1.

In summary, the current study demonstrates for the first time that H_2S is vital in maintaining normal EPC angiogenic function and that an H_2S donor can accelerate wound healing in type 2 diabetic mice. These effects of H_2S are related to restoring the angiogenic functions of EPCs by upregulating Ang-1 expression. The findings that an H_2S donor can amend EPC function and improve skin wound recovery may lead to novel therapeutic strategies for diabetic vascular complications and diabetic skin ulcerations.

Acknowledgments. The authors thank Drs. Patricia Loughran, Jie-Mei Wang, and Mingwei Zhang for their technical support.

Funding. This work was supported in part by the National Basic Research Program (973 Program) 2014CB542400 and the National Science Foundation of China (81130004, 81370359, and 913392019 to A.F.C.; 81070650 and 81270397 to F.L.; 30900519 and 81370429 to D.-D.C.). Support was also received from Shanghai Jiao Tong University Affiliated Sixth People's Hospital Fellowship to F.L.

Duality of Interest. No potential conflicts of interest relevant to this article were reported.

Author Contributions. F.L. and D.-D.C. designed the experiments, conducted the in vitro cell functional tests and the in vivo cell therapy, and wrote the manuscript. X.S. and H.-H.X. performed the Western blot on patient skin samples. H.Y. conducted the in vitro cell biochemical tests and contributed to discussion. W.J. and A.F.C. designed the study, contributed to discussion, and reviewed and edited the manuscript. F.L., D.-D.C., and A.F.C. are the guarantors of this work and, as such, had full access to all the data in the study and take responsibility for the integrity of the data and the accuracy of the data analysis.

References

1. Icks A, Haastert B, Trautner C, Giani G, Glaeske G, Hoffmann F. Incidence of lower-limb amputations in the diabetic compared to the non-diabetic population. findings from nationwide insurance data, Germany, 2005-2007. Exp Clin Endocrinol Diabetes 2009;117:500–504

2. Velazquez OC. Angiogenesis and vasculogenesis: inducing the growth of new blood vessels and wound healing by stimulation of bone marrow-derived progenitor cell mobilization and homing. J Vasc Surg 2007;45 (Suppl. A):A39–A47.

3. Brem H, Tomic-Canic M. Cellular and molecular basis of wound healing in diabetes. J Clin Invest 2007;117:1219–1222

4. Fiorina P, Pietramaggiori G, Scherer SS, et al. The mobilization and effect of endogenous bone marrow progenitor cells in diabetic wound healing. Cell Transplant 2010;19:1369–1381

5. Fadini GP, Miorin M, Facco M, et al. Circulating endothelial progenitor cells are reduced in peripheral vascular complications of type 2 diabetes mellitus. J Am Coll Cardiol 2005;45:1449–1457

6. Albiero M, Menegazzo L, Boscaro E, Agostini C, Avogaro A, Fadini GP. Defective recruitment, survival and proliferation of bone marrow-derived progenitor cells at sites of delayed diabetic wound healing in mice. Diabetologia 2011;54:945–953

7. Loomans CJ, de Koning EJ, Staal FJ, et al. Endothelial progenitor cell dysfunction: a novel concept in the pathogenesis of vascular complications of type 1 diabetes. Diabetes 2004;53:195–199

8. Singh AK, Gudehithlu KP, Patri S, et al. Impaired integration of endothelial progenitor cells in capillaries of diabetic wounds is reversible with vascular endothelial growth factor infusion. Transl Res 2007;149:282–291

9. Li L, Hsu A, Moore PK. Actions and interactions of nitric oxide, carbon monoxide and hydrogen sulphide in the cardiovascular system and in inflammation—a tale of three gases! Pharmacol Ther 2009;123:386–400

10. Renga B. Hydrogen sulfide generation in mammals: the molecular biology of cystathionine-β-synthase (CBS) and cystathionine-γ-lyase (CSE). Inflamm Allergy Drug Targets 2011;10:85–91

11. Wang MJ, Cai WJ, Zhu YC. Mechanisms of angiogenesis: role of hydrogen sulphide. Clin Exp Pharmacol Physiol 2010;37:764–771

12. Schleifenbaum J, Köhn C, Voblova N, et al. Systemic peripheral artery relaxation by KCNQ channel openers and hydrogen sulfide. J Hypertens 2010;28:1875–1882

13. Yang G, Wu L, Jiang B, et al. H2S as a physiologic vasorelaxant: hypertension in mice with deletion of cystathionine gamma-lyase. Science 2008;322:587–590

14. Wagner CA. Hydrogen sulfide: a new gaseous signal molecule and blood pressure regulator. J Nephrol 2009;22:173–176

15. Henderson PW, Singh SP, Belkin D, et al. Hydrogen sulfide protects against ischemia-reperfusion injury in an in vitro model of cutaneous tissue transplantation. J Surg Res 2010;159:451–455

16. Osipov RM, Robich MP, Feng J, et al. Effect of hydrogen sulfide in a porcine model of myocardial ischemia-reperfusion: comparison of different administration regimens and characterization of the cellular mechanisms of protection. J Cardiovasc Pharmacol 2009;54:287–297

17. Bucci M, Cirino G. Hydrogen sulphide in heart and systemic circulation. Inflamm Allergy Drug Targets 2011;10:103–108

18. Yang G, Wu L, Bryan S, Khaper N, Mani S, Wang R. Cystathionine gamma-lyase deficiency and overproliferation of smooth muscle cells. Cardiovasc Res 2010;86:487–495

19. Brancaleone V, Roviezzo F, Vellecco V, De Gruttola L, Bucci M, Cirino G. Biosynthesis of H2S is impaired in non-obese diabetic (NOD) mice. Br J Pharmacol 2008;155:673–680

20. Jain SK, Bull R, Rains JL, et al. Low levels of hydrogen sulfide in the blood of diabetes patients and streptozotocin-treated rats causes vascular inflammation? Antioxid Redox Signal 2010;12:1333–1337

21. Wallace JL, Dicay M, McKnight W, Martin GR. Hydrogen sulfide enhances ulcer healing in rats. FASEB J 2007;21:4070–4076

22. Papapetropoulos A, Pyriochou A, Altaany Z, et al. Hydrogen sulfide is an endogenous stimulator of angiogenesis. Proc Natl Acad Sci U S A 2009;106:21972–21977

23. Cai WJ, Wang MJ, Moore PK, Jin HM, Yao T, Zhu YC. The novel proangiogenic effect of hydrogen sulfide is dependent on Akt phosphorylation. Cardiovasc Res 2007;76:29–40

24. Thomas M, Augustin HG. The role of the angiopoietins in vascular morphogenesis. Angiogenesis 2009;12:125–137
25. Chen JX, Stinnett A. Disruption of Ang-1/Tie-2 signaling contributes to the impaired myocardial vascular maturation and angiogenesis in type II diabetic mice. Arterioscler Thromb Vasc Biol 2008;28:1606–1613
26. Lim HS, Blann AD, Chong AY, Freestone B, Lip GY. Plasma vascular endothelial growth factor, angiopoietin-1, and angiopoietin-2 in diabetes: implications for cardiovascular risk and effects of multifactorial intervention. Diabetes Care 2004;27:2918–2924
27. Chen YH, Lin SJ, Lin FY, et al. High glucose impairs early and late endothelial progenitor cells by modifying nitric oxide-related but not oxidative stress-mediated mechanisms. Diabetes 2007;56:1559–1568
28. Bao P, Kodra A, Tomic-Canic M, Golinko MS, Ehrlich HP, Brem H. The role of vascular endothelial growth factor in wound healing. J Surg Res 2009;153:347–358
29. Brem H, Kodra A, Golinko MS, et al. Mechanism of sustained release of vascular endothelial growth factor in accelerating experimental diabetic healing. J Invest Dermatol 2009;129:2275–2287
30. Stephenson K, Tunstead J, Tsai A, Gordon R, Henderson S, Dansky HM. Neointimal formation after endovascular arterial injury is markedly attenuated in db/db mice. Arterioscler Thromb Vasc Biol 2003;23:2027–2033
31. Sivarajah A, McDonald MC, Thiemermann C. The production of hydrogen sulfide limits myocardial ischemia and reperfusion injury and contributes to the cardioprotective effects of preconditioning with endotoxin, but not ischemia in the rat. Shock 2006;26:154–161
32. Wang MJ, Cai WJ, Li N, Ding YJ, Chen Y, Zhu YC. The hydrogen sulfide donor NaHS promotes angiogenesis in a rat model of hind limb ischemia. Antioxid Redox Signal 2010;12:1065–1077
33. Zhang J, Sio SW, Moochhala S, Bhatia M. Role of hydrogen sulfide in severe burn injury-induced inflammation in mice. Mol Med 2010;16:417–424
34. Gao Y, Yao X, Zhang Y, et al. The protective role of hydrogen sulfide in myocardial ischemia-reperfusion-induced injury in diabetic rats. Int J Cardiol 2011;152:177–183
35. Marrotte EJ, Chen DD, Hakim JS, Chen AF. Manganese superoxide dismutase expression in endothelial progenitor cells accelerates wound healing in diabetic mice. J Clin Invest 2010;120:4207–4219
36. Luo JD, Wang YY, Fu WL, Wu J, Chen AF. Gene therapy of endothelial nitric oxide synthase and manganese superoxide dismutase restores delayed wound healing in type 1 diabetic mice. Circulation 2004;110:2484–2493
37. Zhuo Y, Chen PF, Zhang AZ, Zhong H, Chen CQ, Zhu YZ. Cardioprotective effect of hydrogen sulfide in ischemic reperfusion experimental rats and its influence on expression of survivin gene. Biol Pharm Bull 2009;32:1406–1410
38. Lou LX, Geng B, Du JB, Tang CS. Hydrogen sulphide-induced hypothermia attenuates stress-related ulceration in rats. Clin Exp Pharmacol Physiol 2008;35:223–228
39. Ang SF, Moochhala SM, Bhatia M. Hydrogen sulfide promotes transient receptor potential vanilloid 1-mediated neurogenic inflammation in polymicrobial sepsis. Crit Care Med 2010;38:619–628
40. Zhao T, Li J, Chen AF. MicroRNA-34a induces endothelial progenitor cell senescence and impedes its angiogenesis via suppressing silent information regulator 1. Am J Physiol Endocrinol Metab 2010;299:E110–E116
41. Bae ON, Wang JM, Baek SH, Wang Q, Yuan H, Chen AF. Oxidative stress-mediated thrombospondin-2 upregulation impairs bone marrow-derived angiogenic cell function in diabetes mellitus. Arterioscler Thromb Vasc Biol 2013;33:1920–1927
42. Elsey DJ, Fowkes RC, Baxter GF. Regulation of cardiovascular cell function by hydrogen sulfide (H(2)S). Cell Biochem Funct 2010;28:95–106
43. Chen AF, Chen DD, Daiber A, et al. Free radical biology of the cardiovascular system. Clin Sci (Lond) 2012;123:73–91
44. Chen DD, Dong YG, Yuan H, Chen AF. Endothelin 1 activation of endothelin A receptor/NADPH oxidase pathway and diminished antioxidants critically contribute to endothelial progenitor cell reduction and dysfunction in salt-sensitive hypertension. Hypertension 2012;59:1037–1043
45. Wang JM, Tao J, Chen DD, et al. MicroRNA miR-27b rescues bone marrow-derived angiogenic cell function and accelerates wound healing in type 2 diabetes mellitus. Arterioscler Thromb Vasc Biol 2014;34:99–109
46. Joo HJ, Kim H, Park SW, et al. Angiopoietin-1 promotes endothelial differentiation from embryonic stem cells and induced pluripotent stem cells. Blood 2011;118:2094–2104
47. Jiraritthamrong C, Kheolamai P, U-Pratya Y, et al. In vitro vessel-forming capacity of endothelial progenitor cells in high glucose conditions. Ann Hematol 2012;91:111–320
48. Fujiyama S, Matsubara H, Nozawa Y, et al. Angiotensin AT(1) and AT(2) receptors differentially regulate angiopoietin-2 and vascular endothelial growth factor expression and angiogenesis by modulating heparin binding-epidermal growth factor (EGF)-mediated EGF receptor transactivation. Circ Res 2001;88:22–29
49. Augustin HG, Koh GY, Thurston G, Alitalo K. Control of vascular morphogenesis and homeostasis through the angiopoietin-Tie system. Nat Rev Mol Cell Biol 2009;10:165–177
50. Köhn C, Dubrovska G, Huang Y, Gollasch M. Hydrogen sulfide: potent regulator of vascular tone and stimulator of angiogenesis. Int J Biomed Sci 2012;8:81–86
51. Szabó C, Papapetropoulos A. Hydrogen sulphide and angiogenesis: mechanisms and applications. Br J Pharmacol 2011;164:853–865